

Performance of Nano-Hydroxyapatite/ Beta-Tricalcium Phosphate and Xenogenic Hydroxyapatite on Bone Regeneration in Rat Calvarial Defects: Histomorphometric, Immunohistochemical and Ultrastructural Analysis

Igor da Silva Brum, Lucio Frigo, Paulo Goncalo Pinto dos Santos, Carlos Nelson Elias, Guilherme Aparecido Monteiro Duque da Fonseca & Jorge Jose de Carvalho

To cite this article: Igor da Silva Brum, Lucio Frigo, Paulo Goncalo Pinto dos Santos, Carlos Nelson Elias, Guilherme Aparecido Monteiro Duque da Fonseca & Jorge Jose de Carvalho (2021) Performance of Nano-Hydroxyapatite/Beta-Tricalcium Phosphate and Xenogenic Hydroxyapatite on Bone Regeneration in Rat Calvarial Defects: Histomorphometric, Immunohistochemical and Ultrastructural Analysis, International Journal of Nanomedicine, , 3473-3485, DOI: [10.2147/IJN.S301470](https://doi.org/10.2147/IJN.S301470)

To link to this article: <https://doi.org/10.2147/IJN.S301470>



© 2021 da Silva Brum et al.



Published online: 18 May 2021.



Submit your article to this journal [↗](#)



Article views: 218



View related articles [↗](#)




View Crossmark data [↗](#)



Citing articles: 5 View citing articles [↗](#)

Performance of Nano-Hydroxyapatite/Beta-Tricalcium Phosphate and Xenogenic Hydroxyapatite on Bone Regeneration in Rat Calvarial Defects: Histomorphometric, Immunohistochemical and Ultrastructural Analysis

Igor da Silva Brum ¹

Lucio Frigo ²

Paulo Goncalo Pinto dos Santos¹

Carlos Nelson Elias ³

Guilherme Aparecido

Monteiro Duque da Fonseca²

Jorge Jose de Carvalho⁴

¹Implantology Department, School of Dentistry, Universidade do Estado do Rio de Janeiro, Rio de Janeiro, Brazil;

²Periodontology Department, School of Dentistry, Universidade Guarulhos, São Paulo, Brazil; ³Instituto Militar de Engenharia, Rio de Janeiro, Brazil;

⁴Biology Department, School of Medicine, Universidade do Estado do Rio de Janeiro, Rio de Janeiro, Brazil

Background: Synthetic biomaterials have played an increasingly prominent role in the substitution of naturally derived biomaterials in current surgery practice. In vitro and in vivo characterization studies of new synthetic biomaterials are essential to analyze their physico-chemical properties and the underlying mechanisms associated with the modulation of the inflammatory process and bone healing.

Purpose: This study compares the in vivo tissue behavior of a synthetic biomaterial nano-hydroxyapatite/beta-tricalcium phosphate (nano-HA/ β -TCP mixture) and deproteinized bovine bone mineral (DBBM) in a rat calvarial defect model. The innovation of this work is in the comparative analysis of the effect of new synthetic and commercially xenogenic biomaterials on the inflammatory response, bone matrix gain, and stimulation of osteoclastogenesis and osteoblastogenesis.

Methods: Both biomaterials were inserted in rat defects. The animals were divided into three groups, in which calvarial defects were filled with xenogenic biomaterials (group 1) and synthetic biomaterials (group 2), or left unfilled (group 3, controls). Sixty days after calvarial bone defects filled with biomaterials, periodic acid Schiff (PAS) and Masson's trichrome staining, immunohistochemistry tumor necrosis factor- α (TNF- α), matrix metalloproteinase-9 (MMP-9), and electron microscopy analyses were conducted.

Results: Histomorphometric analysis revealed powerful effects such as a higher amount of proteinaceous matrix and higher levels of TNF- α and MMP-9 in bone defects treated with alloplastic nano-HA/ β -TCP mixture than xenogenic biomaterial, as well as collagen-proteinaceous material in association with hydroxyapatite crystalloids.

Conclusion: These data indicate that the synthetic nano-HA/ β -TCP mixture enhanced bone formation/remodeling in rat calvarial bone defects. The nano-HA/ β -TCP did not present risks of cross-infection/disease transmission. The synthetic nano-hydroxyapatite/beta-tricalcium phosphate mixture presented adequate properties for guided bone regeneration and guided tissue regeneration for dental surgical procedures.

Keywords: biomaterial, hydroxyapatite, beta-tricalcium phosphate, bone healing, histomorphometry

Correspondence: Lucio Frigo
Periodontology Department, School of Dentistry, Universidade Guarulhos, Praça Teresa Cristina, 01, Guarulhos, São Paulo, 07023-070, Brazil
Tel/Fax +55-11- 2464-1684
Email luciofrigo@uol.com.br

Introduction

Synthetic biomaterials play a pivotal role in tissue engineering and have been applied in a wide variety of therapeutic strategies. As new synthetic biomaterials are developed, it is essential to analyze the behavior of proteins and cells at the biomaterial–tissue interface. Synthetic biomaterials have been developed for guided bone regeneration and guided tissue regeneration applications for dental surgical procedures. The use of natural and synthetic biomaterial influences osteoblastic and osteoclastic cell activities that enhance bone extracellular matrix production or induces bone resorption (Figure 1). By controlling the chemical composition, physical, mechanical properties of biomaterials, it is possible to obtain adequate control of their capacity to actively modulate cells and lead to the formation of bone tissue. Crystallinity, porosity, nanometric structure, particles size, percentage of hydroxyapatite (HA), and percentage of beta-tricalcium phosphate (β -TCP) are synthetic biomaterial characteristics that influence bone healing.¹ HA has been used as a bone substitute for years and has yielded promising results. HA has low absorption rates and high predictability concerning the osteoconductive potential of enhancing bone healing and bone tissue adapting.²

Irrespective β -TCP did not be detected in mammalian bone, β -TCP has similarities to bone mineral phase³ and is commonly used for guided bone regeneration with biodegradation and absorption faster than other bioceramics. The β -TCP has low mechanical resistance and complex biosynthesis that are some drawbacks.⁴ Nano-HA/ β -TCP mixture in varying proportions would improve the faster neo-formed properties of β -TCP with the long absorption time of HA to

maintain graft site tissue volume.⁵ The more efficient HA/ β -TCP proportion studies have ascertained how HA nanometric structure improves the bone-forming process. Particles with nanometric size have suitable characteristics such as larger surface area and interfacial compatibility than micrometric particles. Nanometric biomaterial particles provide better cell-to-cell interactions, increase adhesion, migration, proliferation, and differentiation than micrometric particles.^{6,7} Literature result has been shown that nano-HA/ β -TCP particles mixture is more efficient in promoting vascularization in bone healing than pure HA or β -TCP.¹

The relationship of matrix metalloproteinases (MMP), in particular MMP-9, with bone remodeling has received great attention recently.⁸ MMP-9 is expressed in osteoblasts and osteoclasts and can degrade extracellular fibrillar components, mainly partially hydrolyzed collagen and $\alpha 2$ chains of type I collagen.⁹ Diffusely MMP-9-immunolabelled in bone matrix suggests bone-remodeling.¹⁰ Tumor necrosis factor-alpha (TNF- α) is a cell-signaling mediator, also involved in bone metabolism. In mature osteoblasts, TNF- α inhibits gene expression of substances related to bone matrix production and induces osteoclastogenesis-related genes.^{11,12}

In virtue of the scarce number of researches evaluating nano-HA/ β -TCP mixture, the objective of this experimental study was to compare the behavior of nano-HA/ β -TCP mixture and commercially available deproteinized bovine bone mineral (DBBM) biomaterial. Both materials are inserted in rat calvarial defects. The histomorphometric analysis has been done using Masson's trichrome and Periodic Acid Schiff (PAS) staining, in addition to TNF- α and MMP-9 immunostaining testing. The biomaterials

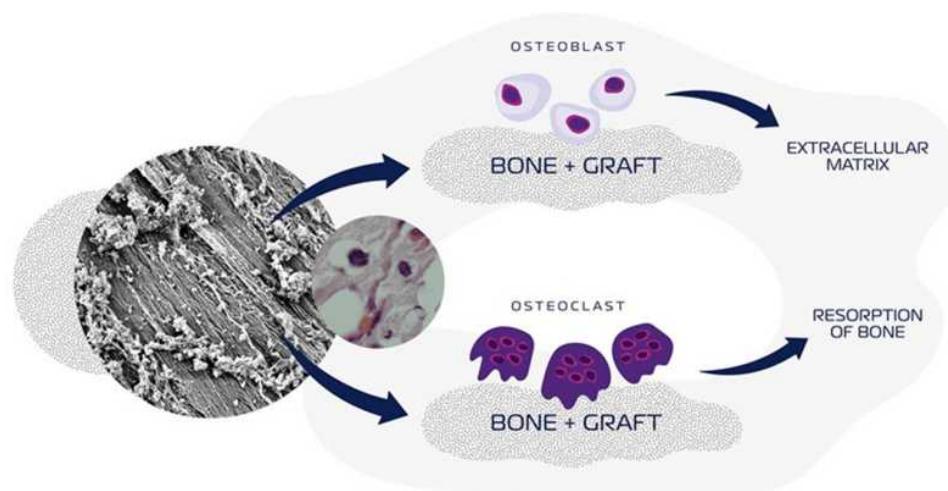


Figure 1 Schematic illustration of a synthetic-HA and/or β -TCP-based biomaterials influences bone deposition, osteoblast activities, bone resorption, and osteoclast activities.

morphologies were characterized by scanning electron microscopy.

Materials and Methods

Biomaterials

The *in vivo* behavior of two biomaterials was compared. One of them was a commercially available (xenogenic biomaterial), which is a deproteinized bovine bone material named Bio-Oss® (Geistlich Pharma AG, Wolhusen, Switzerland). The second analyzed biomaterial was a synthesized (alloplastic biomaterial) mixture of nanometric particle size of hydroxyapatite and β -TCP (80/20%). The alloplastic biomaterial mixture was synthesized and named Blue Bone® at facilities of Regener Biomateriais Co (Curitiba, Brazil). Figure 2 shows the nanometric particles of hydroxyapatite and β -TCP morphologies used in the alloplastic biomaterial mixture.

Animals

Thirty-six adult male Wistar rats, weighing 200–220 g, provided by Instituto de Biologia Roberto Alcântara Central Animal Facility at Universidade Estadual do Rio de Janeiro (Brazil), was used. Rats were housed individually in cages with free access to food and water. Twelve-hour light/dark cycle (7:00 AM/7:00 PM) was set and a 22°C temperature was kept constant. Animals were randomly divided into three groups, with 12 animals in each group. Institutional and national guide for the care and use of laboratory animals were followed. All

experimental procedures and drug administration were approved by Universidade Estadual do Rio de Janeiro Ethics Committee for Animal Care (#001/2019).

Calvarial Bone Defects

Animals received xylazine/ketamine hydrochloride solution (1/1, 0.1mg/kg, intraperitoneally [i.p.]) as anesthetics. Two sagittal incisions were made in a previously trichotomized dorsal cranium using a sterile surgical scalp. Superficial tissue and periosteum in the parietal region were cleared bilaterally to provide enough area to bone defects, for which a sterilized punch (cutting edge Ø 3mm) was used. Extraction of bone remains was made carefully to avoid duramater and related blood vessel damage. One defect in each animal was filled with biomaterial and one defect was left unfilled. One bone defect in 12 animals was filled with deproteinized bovine bone mineral Bio-Oss® biomaterial and an equal animals number received nano-HA/ β -TCP (80/20%) mixture (Blue Bone®). Twelve animals did not receive any biomaterial and served as a control group. Cotton-wire sutures were used for the closure of the incision.

Sixty days after surgery and placement of biomaterials, animals were euthanized under deep anesthesia with xylazine/ketamine hydrochloride solution (1/1, 0.3mg/kg, i.p.). Animal heads were separated from the body and trimmed for decalcification in EDTA/phosphate-buffered saline (PBS) (7.0%, 0.1M, pH 7.4) for

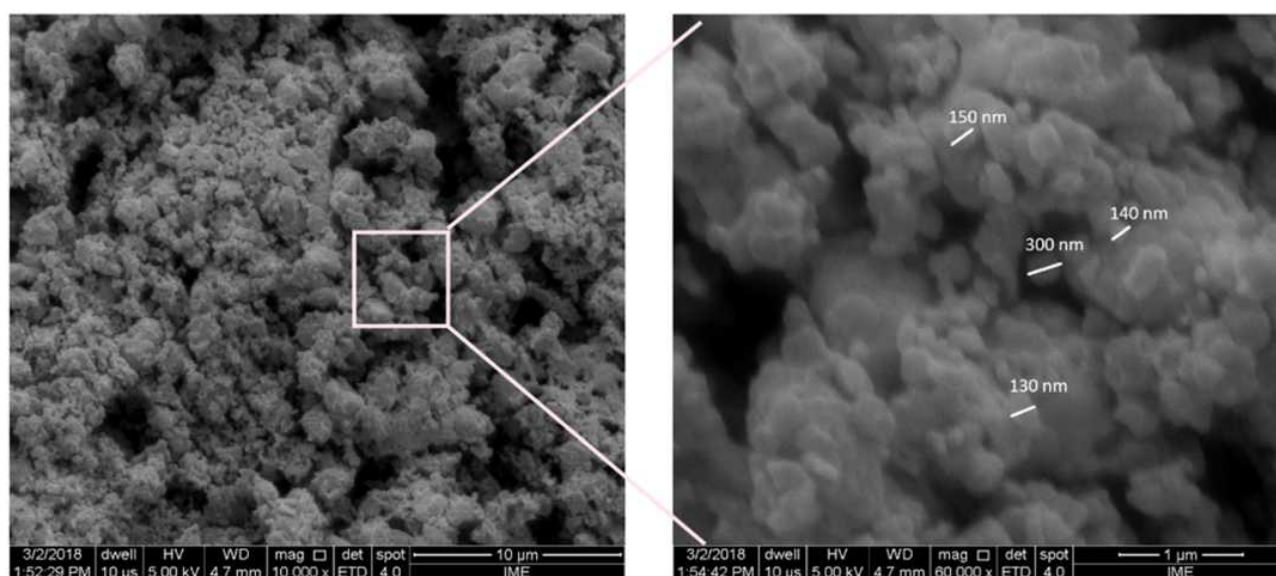


Figure 2 Scanning electron photomicrography showing nano-HA/ β -TCP mixture with particles size from 130 to 300nm. X 10,000, X 60,000.

forty days. Prepared specimens were rinsed in distilled water, dehydrated using different grades of alcohol (70%, 95%, 100%), and rinsed in dimethyl benzene for paraffin embedding at 65°C. Seven-micrometer thick samples were cut with the LEICA microtome (LEICA, Nussloch, Germany).

Masson's Trichrome, Periodic Acid Schiff (PAS), and Immunohistochemistry

For Masson's trichrome-staining protocol, slides were deparaffinized and rehydrated through 100%, 90%, and 70% alcohol, washed in distilled water, and stained in Weigert's iron hematoxylin solution for 10 min. After being washed in distilled water, slides were stained in Biebrich scarlet-acid fuchsin solution for 10–15 min, washed again in distilled water, differentiated in the phosphomolybdic-phosphotungstic acid solution for 10–15 min, stained with aniline blue solution for 5 min, washed with distilled water, dehydrated, and mounted with resinous mounting medium.

According to the periodic acid Schiff (PAS) protocol recommendations, slides were stained in periodic acid (1%) for 5 min, washed in distilled water, stained in Schiff's fuchsin-sulfite reagent for 5–15 min, washed under running tap water for 5–10 min, and counterstained with hematoxylin for 15 min.

For the protocol used in immunohistochemistry, slides were deparaffinized, rehydrated, and immersed in hydrogen peroxide (3%) to neutralize endogenous peroxidase for 15 min. Histological sections were previously rinsed in PBS and submitted citrate buffer solution (pH 6.0) and heated (60°C) for 20 min to achieve antigen retrieval. Sections followed a PBS-containing (3%) bovine serum albumin rinse for 20 min to address antigen cross-reaction. After that, incubation with primary-antibody, anti-MMP-9 (1:200) (Santa Cruz Biotechnology, USA), and TNF- α (1:200) (Santa Cruz Biotechnology, USA) in a humidified chamber at 4°C overnight was conducted. Sections were, finally, incubated with VECTASTAIN® Universal Quick HRP kit detection system, revealed with DAB (3,3-diaminobenzidine), and counterstained with hematoxylin.

Three randomized slide fields in PAS, Masson's trichrome-stained, MMP-9, and TNF- α immune-stained were selected by a researcher unaware of the groups tested (Figure 3). Images were captured in a Carl Zeiss photomicroscope (Carl Zeiss – JVCTK-1270) at X 400

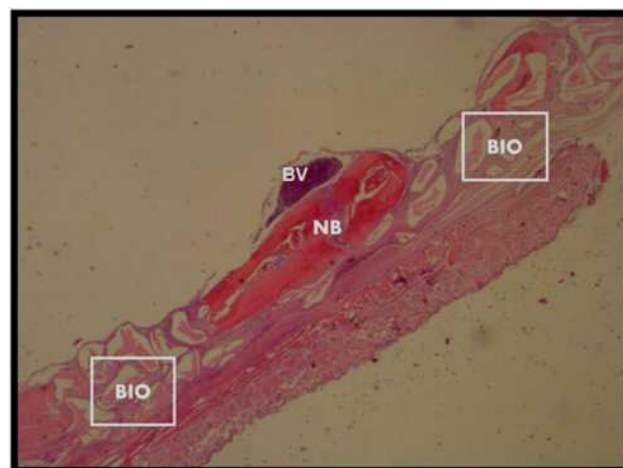


Figure 3 Calvarial samples analyzed sixty days after surgery. X 25 magnification. **Abbreviations:** BIO, biomaterial; NB, native bone; BV, blood vessel.

magnification. GraphPad Prism (8.0 version) was used to image quantification. Pink-stained areas in PAS and blue-stained areas in Masson's trichrome were set for quantification. In immune-stained slides (MMP-9 and TNF- α) brownish deposits were considered immune-marked for quantification. Quantification was based on measuring the area of the selected color set in the GraphPad Prism computer program.

Scanning Electron Microscopy

After periosteum removal, bone defects filled with biomaterials were exposed, before fixation in glutaraldehyde solution (2.5%) in sodium cacodylate buffer (0.1M, pH 7.4) at 48°C for 12 h. Post-fixation procedures started with an osmium tetroxide and potassium ferrocyanide (1.0%, 0.8%, respectively) in a cacodylate buffer (0.1M, pH 7.4) incubation for 1 h in the dark, followed by three sodium cacodylate buffer rinses in distilled water (0.2 M, pH 7.4) for 1 h. Followed sequential ethanol grades (25–100%) rinse for specimen dehydration. Sections were immersed in hexamethyldisilazane for 10 min before placing in an evaporation chamber to get dried. Specimens mount on aluminum stubs were achieved by colloidal silver adhesive (Electron Microscopy Sciences, USA). The critical point was accomplished (Critical Point Dryer – CPD 030, Bal-Tec, Germany) and the specimens were coated with gold film by sputtering (Cool Sputter Coater – SCD 005, Bal-Tec, Germany). Gold-coated specimen surfaces were analyzed using a scanning electron microscope (Quanta 250 FEG, FEI Company, USA). An $\times 5000$ magnification was set for biomaterial homogeneity, $\times 15,000$ magnification

Table 1 Histomorphometric and Immunohistochemical Statistical Analysis

| Variables | Study Groups | | | P values |
|--|---------------|-----------------------|---------------|--|
| | Micro-HA | Nano-HA/ β -TCP | Controls | |
| Histomorphometry (% stained area) | Mean (SD) | Mean (SD) | Mean (SD) | |
| Masson's trichrome | 38.95 (21.82) | 77.65 (13.81) | 17.38 (11.56) | nano-HA/ β -TCP vs micro-HA, $P = 0.04$ nano-HA/ β -TCP vs control, $P = 0.0006$ |
| PAS | 0.49 (0.45) | 33.62 (7.19) | 40.3 (12.34) | nano-HA/ β -TCP vs micro-HA, $P = 0.002$ Controls vs HA, $P = 0.0001$ |
| Immunohistochemistry (% stained area) | | | | |
| MMP-9 | 11.03 (5.19) | 47.87 (4.59) | 9.31 (1.96) | nano-HA/ β -TCP vs micro-HA, $P = 0.002$ nano-HA/ β -TCP vs control, $P = 0.0001$ |
| TNF- α | 28.07 (11.09) | 34.46 (8.63) | 28.64 (15.69) | nano-HA/ β -TCP vs control, $P = 0.03$ |

was set for cell clusters and architecture, and $\times 20,000$ magnification was set for specific cell types.

Statistical Analysis

Results are expressed as mean and standard (SD). Data in the three groups were compared with the Kruskal–Wallis test and Mann–Whitney as the posttest. Statistical significance was set at $P < 0.05$. The GraphPad Prism version 8.0 and BioEstat 5.0 were used for statistical analyses.

Results

Histomorphometric and immunohistochemical results are shown in (Table 1). Masson's trichrome is a traditional staining technique that is composed of aniline blue, among other chemicals. Aniline blue has a strong affinity to basic proteins, notably collagen fibrils. Considering that collagen fibrils are the main organic component of bone matrix, mainly Type I collagen, the blue displayed in the bone matrix suggests a net gain or reduction of

bone matrix (Figure 4A–C). The percentage of the stained area was significantly larger in the rat calvaria defects filled with nano-HA/ β -TCP mixture compared with those filled with DBBM ($P = 0.04$) and controls ($P = 0.0006$) (Figure 5).

PAS staining method is based on the oxidizing potential of the periodic acid, which oxidizes cell compounds that harbors free hydroxyl or amino/alkylamine turning them into dialdehydes. These dialdehydes react to Schiff's reagent, resulting in an insoluble magenta color (Figure 6). PAS technique detected the presence of polysaccharides and polysaccharides-rich compounds, like glycoproteins, proteoglycans glycolipids in the tissues. Glycoproteins and proteoglycans were detected by PAS and found mainly in mineralized tissue.

The percentage of the stained area with PAS was significantly larger in the nano-HA/ β -TCP mixture group than the DBBM group ($P = 0.002$). The control group showed a higher percentage of a stained area

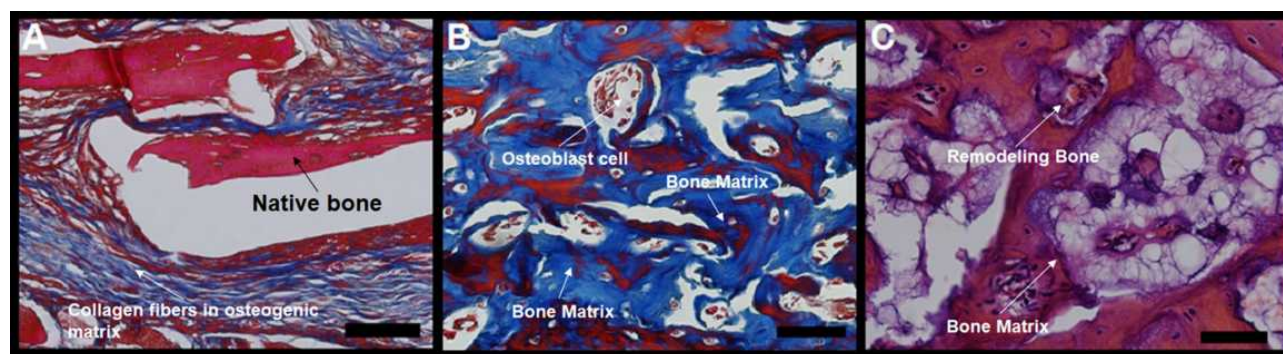


Figure 4 Photomicrographs of slides stained with Masson's trichrome. The bluish color indicates collagen fibrils in the bone matrix. (A) bone defects filled with hydroxyapatite; (B) bone defects filled with nano-hydroxyapatite/ β tricalcium phosphate; (C) unfilled (control). Scale bar 100 μ m, X 400 magnification.

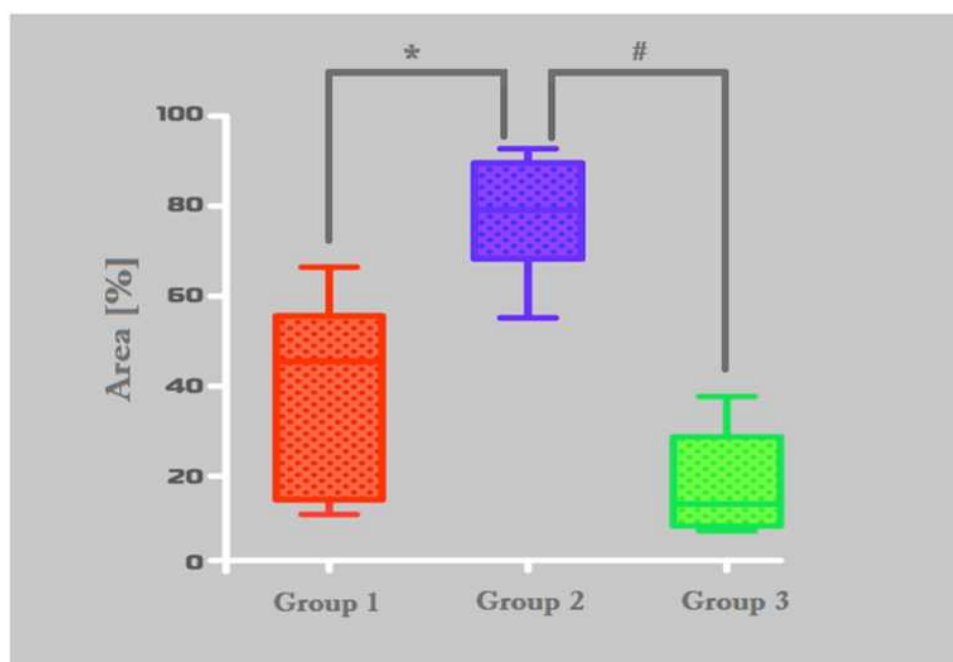


Figure 5 Histomorphometric analysis of Masson's trichrome-stained area results. Group-1 (micro-HA), Group-2 (nano-HA/β-TCP compound) and Group-C (without biomaterial - control). * $p = 0,0043$, # $0,0006$.

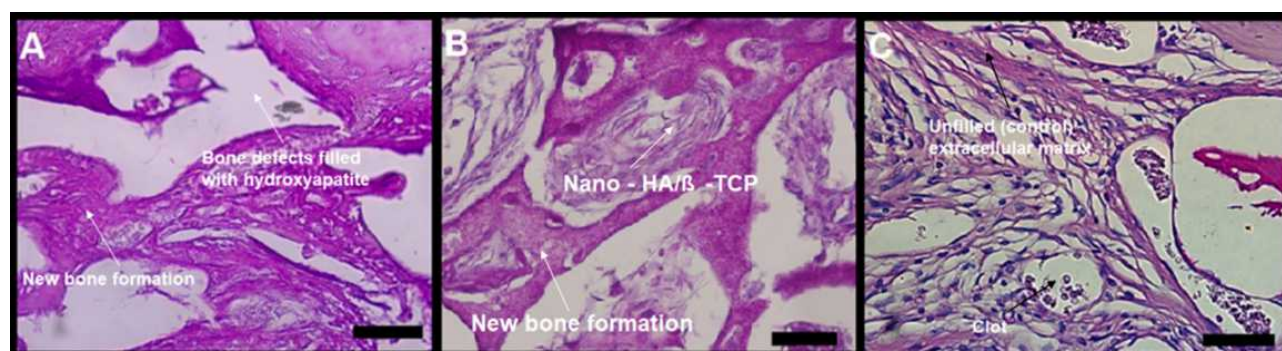


Figure 6 Photomicrographs of slides stained with periodic acid Schiff (PAS). Oxidized hydroxyl and amine/alkylamine chemical groups appear as a magenta-colored complex. The detection of polysaccharides, glycoproteins, and glycolipids suggests new bone formation. (A) bone defects filled with hydroxyapatite; (B) bone defects filled with nano-hydroxyapatite/β tricalcium phosphate; (C) defect without biomaterial (control). Scale bar 100 μm, X 400 magnification.

than the DBBM group ($P = 0.0001$) (Figures 6A–C and 7).

Based on the histomorphometric analysis of Masson's trichrome staining, the Group-2 (nano-HA/β-TCP mixture) showed the highest collagen content. Statistical difference was found between Group-1 (DBBM) and Group-2 (Figure 5).

The histomorphometric analysis of PAS staining results showed that Group-2 (nano-HA/β-TCP mixture) had the highest glycoproteins, polysaccharides, and glycolipids contents. It was also found statistic difference between Group-1 and Group-2 (Figure 7).

Concerning immunohistochemistry, a light brown deposits in bone matrix and inside cells indicated the presence of MMP-9. The percentage of immune-stained areas was significantly higher in bone defects filled with nano-HA/β-TCP mixture than in those filled with micro-HA ($P = 0.002$) or left unfilled (controls) ($P = 0.0001$). No difference was observed between Group-1 (DBBM) and Group-3 (control) (Figures 8A–C and 9).

Light brown deposits in bone matrix and inside cells identified the presence of TNF-α (Figure 10A–C). The percentage of the stained area was significantly higher in the nano-HA/β-TCP mixture group compared with the

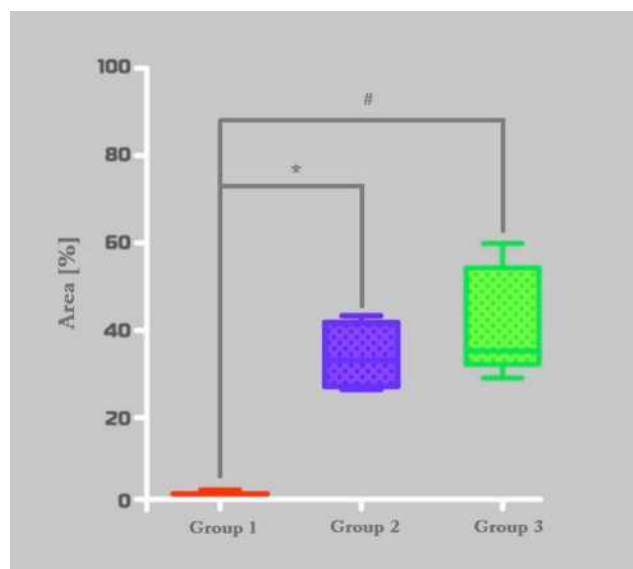


Figure 7 Histomorphometric analysis of PAS stained area. Group-1 (Bio Oss™), Group-2 (Blue Bone™) and Group-C (control). *p = 0,0022, #p = 0,0001.

group of controls defects kept empty ($P = 0.03$). Statistical analysis did not show a significant difference between Group 1 (DBBM) and Group 2 (nano-HA/β-TCP mixture). (Figure 11)

Scanning electron micrographs of nano-HA/β-TCP mixture group showed HA crystals in different shades of blue in contact with protein matrix (Figure 12). These crystals were the junction of HA and glycoproteins. The acicular phase was observed sparsely or combined with diverse types of proteins in the bone matrix, which was suggestive of small diameters collagen fibrils (Figure 13).

Discussion

The analysis of this work used histomorphometry and immunohistochemistry, these methodologies are widely used to assess cell tissue components involved in the

osseointegration and bone remodeling process.^{13–16} The results of the present study showed that the synthetic nano-HA/β-TCP mixture biomaterial used to fill calvarial bone defects in a rat model induced a better cell response than deproteinized bovine bone mineral (DBBM). Nano-HA/β-TCP mixture showed larger percentages of stained areas with Masson's trichrome, PAS, MMP-9, and TNF-α than DBBM biomaterial.

In an in vitro study of nano-HA through the evaluation of cell viability and morphological changes in L-929 mouse fibroblasts cells, no cytotoxic effects were found.¹⁷ In the present study, SEM analysis of a bone defect filled with nano-HA/β-TCP mixture showed a fibroblast possibly acting on the production of extracellular matrix, supposedly to promote tissue healing. Mineralized type I collagen (Coll I) nanofibers, and their nanofibril bundles, are a marked characteristic of the natural bone tissue microstructure.^{18,19} We also observed, in SEM evaluation that images of supposedly collagen fibrils may serve as a scaffold for depositing the bone matrix mineral phase. From this initial process, mineralization deposition proceeds, and a new binding substrate for the cellular and glycoprotein components of the extracellular matrix follows.^{19–21}

Experimental studies have shown that modified grafts can form new bone and integrate into host tissue. However, bone vascularization remains a barrier to be overcome in the case of clinically viable bone graft design and implantation.²² Nano-HA/β-TCP mixture induced a marked increase in vascularization, due to the nano-metric structure that favors angiogenesis.²³ In the present study, the stained area with Masson's trichrome in the nano-HA/β-TCP mixture group was significantly greater than in the DBBM and control groups, supporting the view

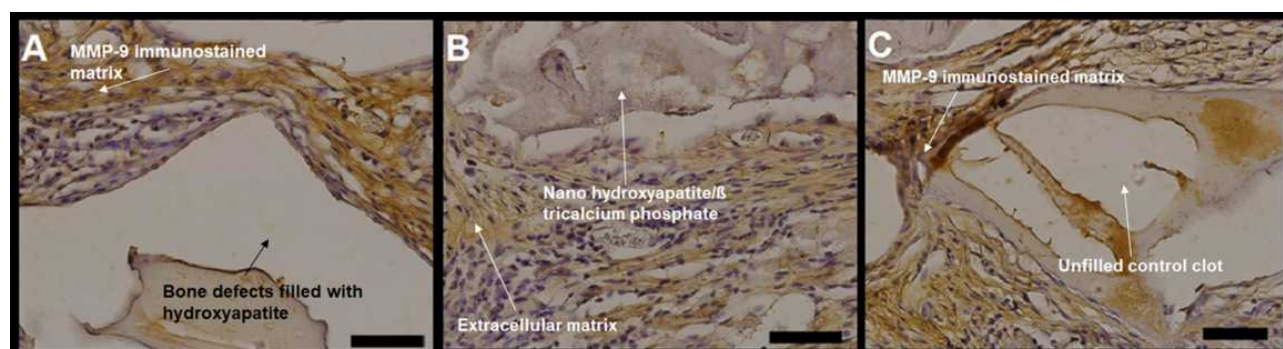


Figure 8 Photomicrographs of MMP-9 immunostained slides, with a light brown color indicating MMP-9. (A) bone defects filled with hydroxyapatite; (B) bone defects filled with nano-hydroxyapatite/β tricalcium phosphate; (C) defect without biomaterial (control). Scale bar 100 μm, X 400 magnification.

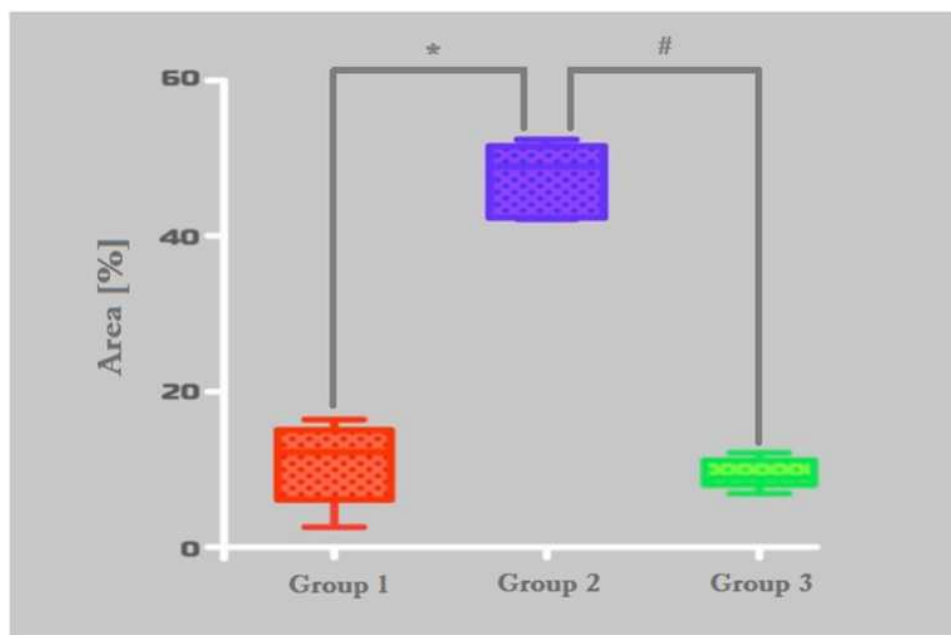


Figure 9 Histomorphometric analysis of MMP-9 stained area. Group-1 (micro-HA), Group-2 (nano-HA/β-TCP compound) and Group-C (control). * $p = 0,0022$, # $0,0001$.

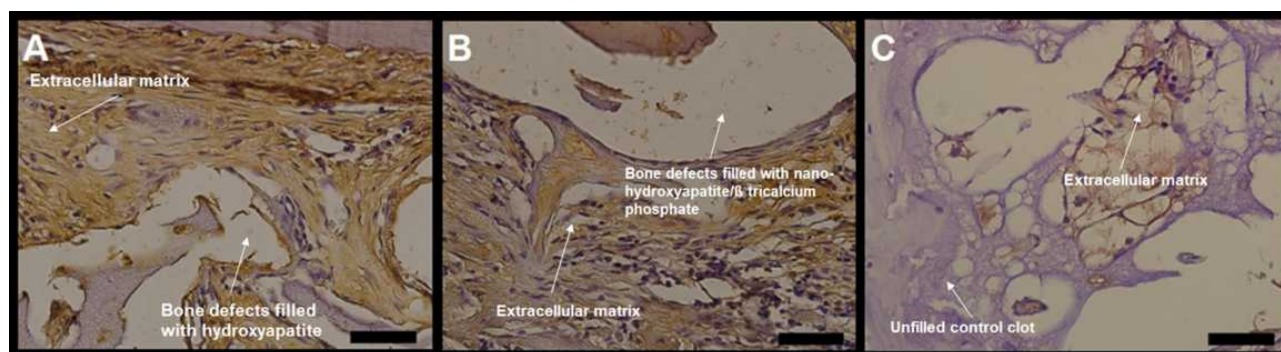


Figure 10 Photomicrographs of TNF- α immunostained slides, with a light brown color indicating the presence of TNF- α . (A) bone defects filled with hydroxyapatite; (B) bone defects filled with nano-hydroxyapatite/β tricalcium phosphate; (C) unfilled (control). Scale bar 100 μ m, X 400 magnification.

that nano-HA/β-TCP mixture may be more efficient in promoting bone matrix collagen synthesis.

Research on MMP-9 has shown beneficial effects on inflammatory processes and bone growth. It was suggested that MMP-9 is deeply involved in bone matrix remodeling and accompanying neovascularization. Moreover, endothelial precursor cells can be recruited from bone marrow by MMP-9.⁸ The results of the present work showed that a higher amount of MMP-9 in bone defects treated with the nano-HA/β-TCP mixture, supporting the view of greater efficiency in bone matrix formation/remodeling than other groups.

This finding is consistent with data reported by other researchers, who found that nano-HA could

enhance TNF- α secretion.²⁴ The nano-HA/β-TCP mixture synthesized in the present work is a promising biomaterial for use in bone regeneration procedures. Nano-HA with different particle particles sizes and crystals could induce changes in cell viability, cytoskeleton, apoptosis, type I collagen, and TNF- α mRNA expression in cultured human osteoblast-like (MG-63) and Macrophage (U937) cell lines.²⁴ Another mechanism for determining the TNF- α is the Receptor Activator of Nuclear factor Kappa-B ligand (RANK-L) which is expressed in osteocytes and regulates osteoclast differentiation. TNF- α is an important RANK-L expression inducer in osteocytes and enhances osteoclastogenesis during the inflammatory

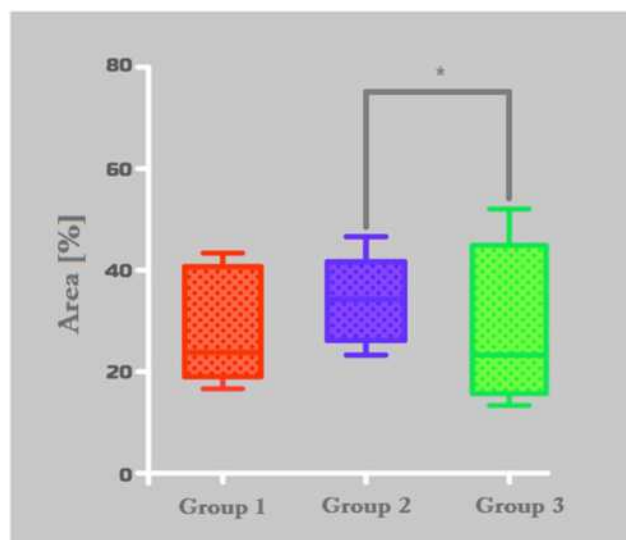


Figure 11 Histomorphometric analysis of TNF- α immunostained area. Group-1 (micro-HA), Group-2 (nano-HA/ β -TCP compound), and Group-3 (control). * $p = 0,0313$.

process.²⁵ TNF- α secretion was related to primed mesenchymal stem cells differentiation to osteoblasts and bone matrix production.^{34,35} The present work results showed that synthetic nano-HA/ β -TCP mixture graft displayed higher TNF- α immunostaining, suggesting a better bone remodeling performance.²⁶

RANK-L increases the differentiation of monocytes in the pre-osteoclast. Immature osteoclasts are also regulated by the RANK/RANK-L to become mature osteoclasts.³⁶ Osteoclasts promote the reabsorption of the fragile fraction of the biomaterial (beta-tricalcium phosphate) until it reaches the resistant fraction (nano-hydroxyapatite), this osteoclastic activity induces Bone Morphogenic Protein (BMP) production and Tumor Growth Factor- β (TGF- β), that activates mesenchymal cells to differentiate into pre-osteoblasts. Immature osteoblasts are induced by the levels of Matrix Metalloproteinase-9 (MMP-9) to differentiate into mature osteoblasts. Osteoblasts start the bone matrix deposition process and increase the levels of Osteoprotegerin (OPG) that act directly in the differentiation of immature osteoclasts through the RANK/RANK-L binding.³⁶ (Figure 14)

Concerning PAS staining, significant differences in favor of the nano-HA/ β -TCP mixture group a faster bone healing process than the DBBM group. In a study on biopsies in human jaws, a new nanoporous-grafting material consisting of nanocrystalline HA embedded in a porous silica gel matrix, showed osteoconductive and biomimetic properties with integration into the host's physiological bone turnover at a very early stage.²⁷ The positive PAS reaction within the material found in our study

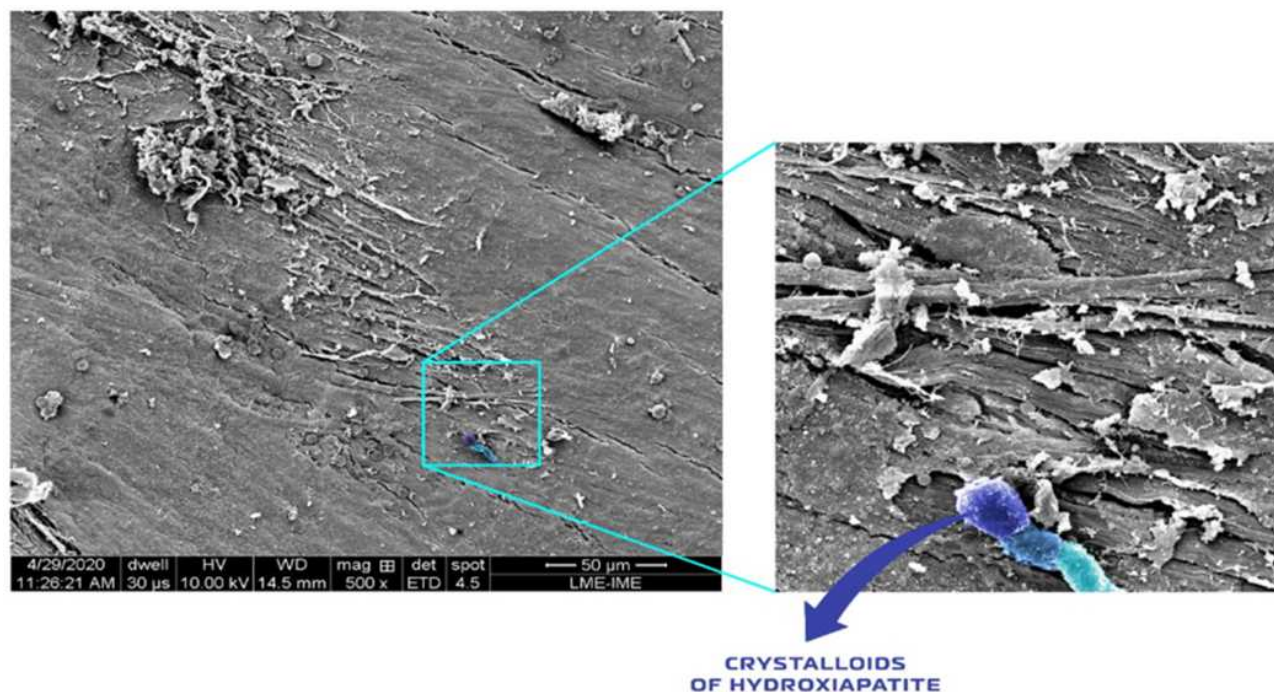


Figure 12 Scanning electron micrographs of bone defects filled with nano-hydroxyapatite/ β tricalcium phosphate showing bone matrix surface, highlighting hydroxyapatite crystals (light and dark blue) in contact with proteinaceous matrix component. Scale bar = 50 μ m, x500 magnification. Magnified image = Scale bar = 20 μ m, X 2375.

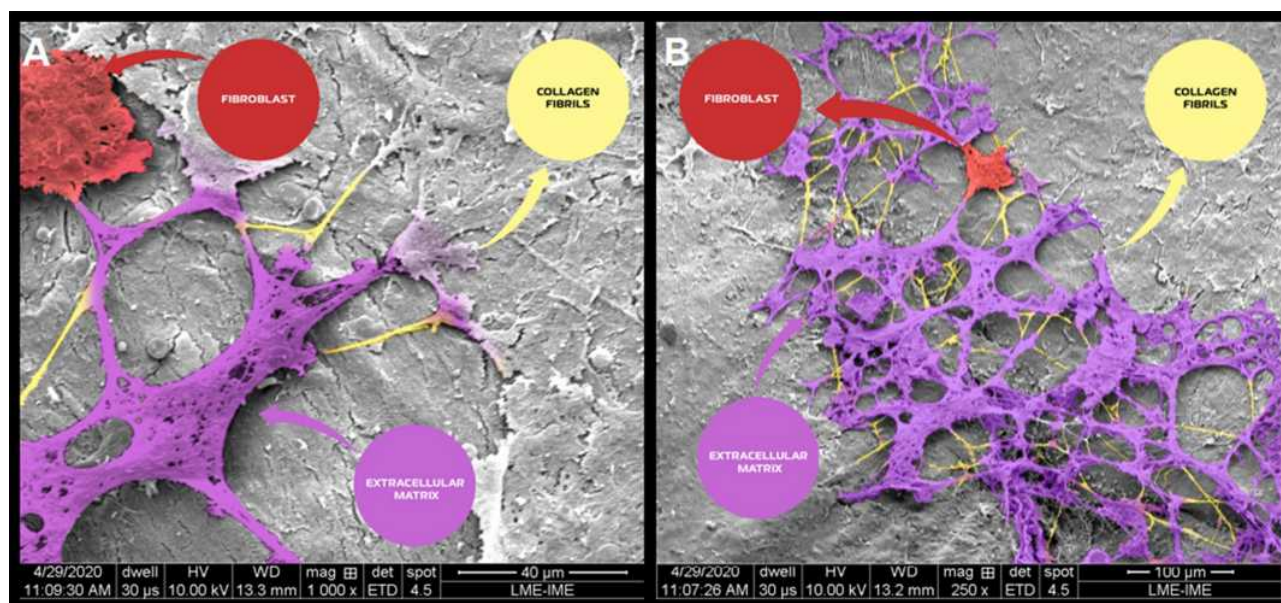


Figure 13 Scanning electron micrographs of bone defects filled with nano-hydroxyapatite/ β tricalcium phosphate showing the surface of the bone matrix. The highlighting images are suggestive of collagen fibrils (yellow), collagen fibrils associated with other types of proteins (magenta) and possibly starting the process of the extracellular matrix formed by an aggregate of glycoproteins and bundles of collagen fibers; and a fibroblast (red). (A) scale bar = 40 μ m, \times 1000; (B) scale bar 100 μ m, \times 250 magnification.

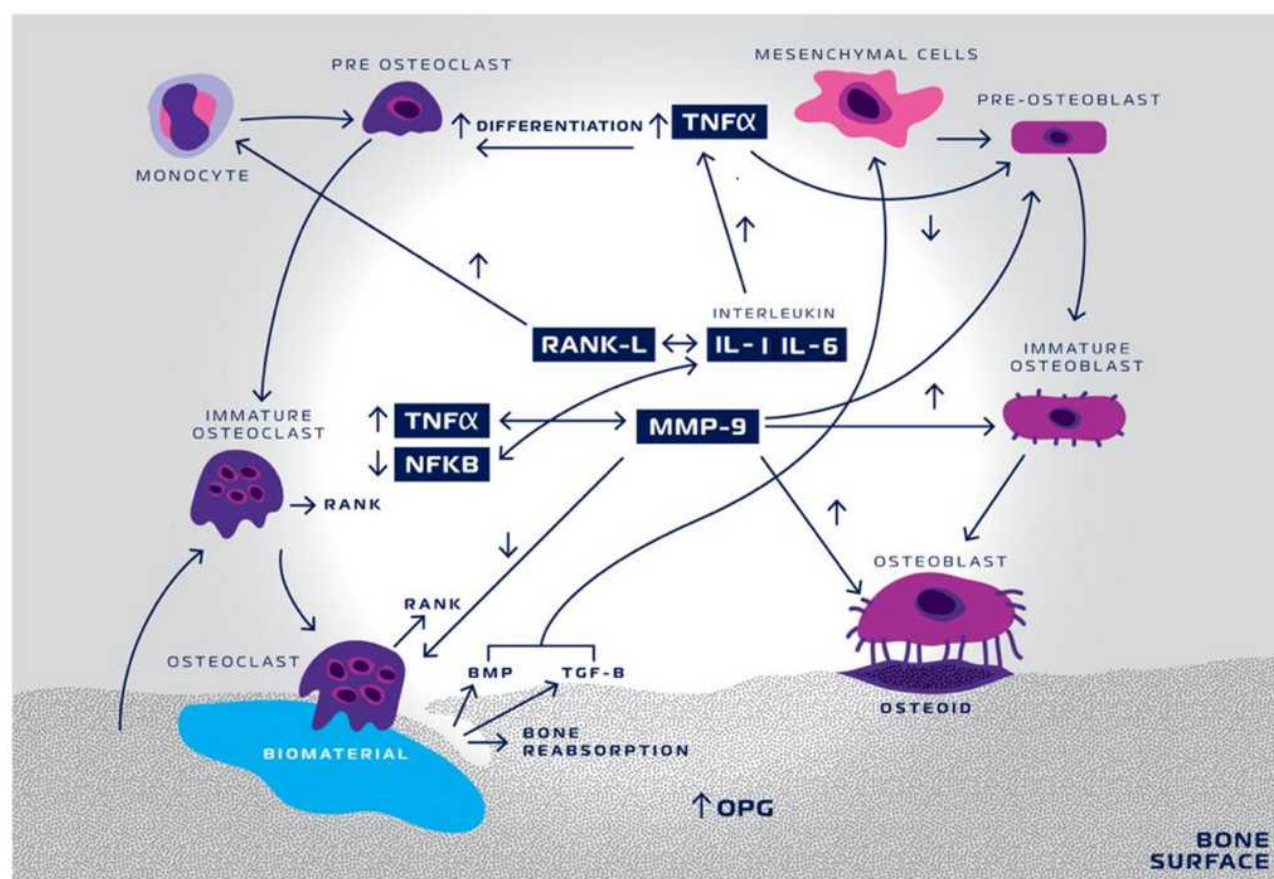


Figure 14 Schematic representation of TNF- α and MMP-9 activity in biomaterial inducing-bone remodeling. Nano-hydroxyapatite/ β -tricalcium phosphate (biomaterial) triggers a cascade of events initiated by tumor necrosis factor- α (TNF- α) increase, activating interleukin-1 (IL-1) and interleukin-6 (IL-6). IL-1 and IL-6 decrease the activity of Nuclear-Factor Kappa-B (NFKB) and consequently increase the activity of the receptor.

indicates glycoproteins, with cell activity was more intense during the first months of graft healing. Other studies have shown similar results.^{28,29}

Different in vivo studies evaluated the cell propagation in calcium phosphate substrates.^{30–32} Noting that there is an increase in the adhesion of mesenchymal stem cells and their spread in β -TCP compared to HA because β -TCP is potentially more osteoinductive compared to HA, while HA is potentially more osteoconductive compared to β -TCP. For this reason, many compounds with more than one phase of calcium phosphate are researched and developed to combine osteoconductive and osteoinductive properties.¹ The determination of the percentage of phases is not yet well defined, although a proportion 80% HA and 20% β -TCP seem adequate because HA is a less resorbable framework than β -TCP, creating an ideal condition, where the reabsorption ratio versus bone matrix deposition keeps itself balanced, generating results in the quality of newly formed bone much more satisfactory than those found in other materials that present substrates of calcium phosphate in different concentrations.³³ The present results support these characteristics with an osteoinductive potential more relevant in the nano-HA/ β -TCP mixture than in the DBBM group.

It is worth mentioning that the presented results are related to a late period of bone healing (60 days) and could be more properly considered as a remodeling process, at least, as far as the nano-HA/ β -TCP mixture is considered. The presence of a higher number of DBBM particles in histological sections suggests that it is experiencing a slower process of healing/remodeling. Besides, evaluation of only two types of mediators (MMP-9, TNF- α) narrows the discussion about cell mechanisms in the healing/remodeling process and demands information obtained from other types of scientific approaches (cell cultures) to add support to the proposed hypothetical mechanism that drives the process. Hence, conclusions based on a late period of bone regeneration and a limited number of cell modulators can be considered limitations of this study and interesting future perspectives.

Conclusion

The results of the study are innovative once they showed that:

- (a) At sub-critical calvarial bone defects (in a rat model) the use of a synthetic nano-HA/ β -TCP biomaterial promoted more favorable bone matrix gain

than a commercially available xenogenic HA, enhanced osteoclastogenesis and osteoblastogenesis by stimulating TNF- α and MMP-9.

- (b) The synthetic nano-HA/ β -TCP biomaterial stimulated new bone formation, as shown by the percentage of PAS stained area on histological studies.
- (c) The electron microscopy analysis showed that the synthetic nano-HA/ β -TCP revealed the presence of HA crystals and collagen fibrils, which are involved in the tissue regeneration process.
- (d) The research showed the powerful effect of a new nanostructured synthetic material that may be suited to maxillary bone filling and maxillary sinus floor augmentation.

Acknowledgments

This research received financial support from the Brazilian Agency CAPES (Coordenação de Aperfeiçoamento de Pessoal de Nível Superior).

Disclosure

The authors report no conflicts of interest in this work.

References

- da Silva Brum I, de Carvalho JJ, da Silva Pires JL, de Carvalho MAA, Dos Santos LBF, Elias CN. Nanosized hydroxyapatite and β -tricalcium phosphate composite: physico-chemical, cytotoxicity, morphological properties and in vivo trial. *Sci Rep*. 2019;9(1):e19602. doi:10.1038/s41598-019-56124-4
- Sudradjat H, Meyer F, Loza K, Eppele M, Enax J. In vivo effects of a hydroxyapatite-based oral care gel on the calcium and phosphorus levels of dental plaque. *Eur J Dent*. 2020;14:206–211. doi:10.1055/s-0040-1708456
- Gupta S, Malhotra A, Jindal R, Garg SK, Kansay R, Mittal N. Role of beta tri-calcium phosphate-based composite ceramic as bone-graft expander in Masquelet's-Induced membrane technique. *Indian J Orthop*. 2019;53:63–69. doi:10.4103/ortho.IJOrtho_240_17
- Titsinides S, Agogiannis G, Karatzas T. Bone grafting materials in dentoalveolar reconstruction: a comprehensive review. *Jpn Dent Sci Rev*. 2019;55:26–32. doi:10.1016/j.jdsr.2018.09.003
- Rasouli R, Barhoum A, Bechelany M, Dufresne A. Nanofibers for biomedical and healthcare applications. *Macromol Biosci*. 2019;19:e1800256. doi:10.1002/mabi.201800256
- Liang W, Ding P, Li G, Lu E, Zhao Z. Hydroxyapatite nanoparticles facilitate osteoblast differentiation and bone formation within sagittal suture during expansion in rats. *Drug Des Devel Ther*. 2021;15:905–917. doi:10.2147/DDDT.S299641
- Ha SW, Jang HL, Nam KT, Beck GR Jr. Nano-hydroxyapatite modulates osteoblast lineage commitment by stimulation of DNA methylation and regulation of gene expression. *Biomaterials*. 2015;65:32–42. doi:10.1016/j.biomaterials.2015.06.039
- Vandooren J, Van den Steen PE, Opdenakker G. Biochemistry and molecular biology of gelatinase B or matrix metalloproteinase-9 (MMP-9): the next decade. *Crit Rev Biochem Mol Biol*. 2013;48:222–272.

9. Grässel S, Beckmann J, Rath B, Vogel M, Grifka J, Tingart M. Expression profile of matrix metalloproteinase-2 and -9 and their endogenous tissue inhibitors in osteonecrotic femoral heads. *Int J Mol Med*. 2010;26:127–133. doi:10.3892/ijmm_00000444
10. Rocha CA, Cestari TM, Vidotti HA, de Assis GF, Garlet GP, Taga R. Sintered anorganic bone graft increases autocrine expression of VEGF, MMP-2 and MMP-9 during repair of critical-size bone defects. *J Mol Histol*. 2014;45(4):447–461. doi:10.1007/s10735-014-9565-4
11. Zhao B. TNF and bone remodeling. *Curr Osteoporos Rep*. 2017;15:126–134. doi:10.1007/s11914-017-0358-z
12. David JP, Schett G. TNF and bone. *Curr Dir Autoimmun*. 2010;11:135–144.
13. Kamitakahara M, Ohtsuki C, Miyazaki T. Review paper: behavior of ceramic biomaterials derived from tricalcium phosphate in physiological condition. *J Biomater Appl*. 2008;23:197–212. doi:10.1177/0885328208096798
14. Solakoglu Ö, Götz W, Heydecke G, Schwarzenbach H. Histological and immunohistochemical comparison of two different allogeneic bone grafting materials for alveolar ridge reconstruction: a prospective randomized trial in humans. *Clin Implant Dent Relat Res*. 2019;21:1002–1016. doi:10.1111/cid.12824
15. Lorenz J, Kubesch A, Al-Maawi S, et al. Allogeneic bone block for challenging augmentation—a clinical, histological, and histomorphometrical investigation of tissue reaction and new bone formation. *Clin Oral Investig*. 2018;22:3159–3169. doi:10.1007/s00784-018-2407-0
16. Pérez-González F, Molinero-Mourelle P, Sánchez-Labrador L, et al. Assessment of clinical outcomes and histomorphometric findings in alveolar ridge augmentation procedures with allogeneic bone block grafts: a systematic review and meta-analysis. *Med Oral Patol Oral Cir Bucal*. 2020;25:e291–e298. doi:10.4317/medoral.23353
17. Szymonowicz M, Korczynski M, Dobrzynski M, et al. Cytotoxicity evaluation of high-temperature annealed nanohydroxyapatite in contact with fibroblast cells. *Materials (Basel)*. 2017;10(6):e590. doi:10.3390/ma10060590
18. Liao S, Ngiam M, Chan CK, Ramakrishna S. Fabrication of nano-hydroxyapatite/collagen/osteonectin composites for bone graft applications. *Biomed Mater*. 2009;4:e025019. doi:10.1088/1748-6041/4/2/025019
19. Ngiam M, Liao S, Patil AJ, Cheng Z, Chan CK, Ramakrishna S. The fabrication of nano-hydroxyapatite on PLGA and PLGA/collagen nanofibrous composite scaffolds and their effects in osteoblastic behavior for bone tissue engineering. *Bone*. 2009;45:4–16. doi:10.1016/j.bone.2009.03.674
20. Tampieri A, Celotti G, Landi E, Sandri M, Roveri N, Falini G. Biologically inspired synthesis of bone-like composite: self-assembled collagen fibers/hydroxyapatite nanocrystals. *J Biomed Mater Res A*. 2003;67:618–625. doi:10.1002/jbm.a.10039
21. Smith LA, Ma PX. Nano-fibrous scaffolds for tissue engineering. *Colloids Surf B Biointerfaces*. 2004;39:125–131. doi:10.1016/j.colsurfb.2003.12.004
22. Fröhlich M, Grayson WL, Wan LQ, Marolt D, Drobic M, Vunjak-Novakovic G. Tissue engineered bone grafts: biological requirements, tissue culture and clinical relevance. *Curr Stem Cell Res Ther*. 2008;3:254–264. doi:10.2174/157488808786733962
23. Amorim Lopes JC, Salviano SH, Antunes Barreto Lins C, Devita RL. Histological and immunohistochemical analysis of a nanobiomaterial in a maxillary sinus lift surgery: a case report. *Br J Med Health Res*. 2020;7(07):13–27.
24. Liu X, Zhao M, Lu J, Ma J, Wei J, Wei S. Cell responses to two kinds of nanohydroxyapatite with different sizes and crystallinities. *Int J Nanomed*. 2012;7:1239–1250.
25. Ohori F, Kitaura H, Marahleh A, et al. Effect of TNF- α -induced sclerostin on osteocytes during orthodontic tooth movement. *J Immunol Res*. 2019;2019:e9716758. doi:10.1155/2019/9716758
26. Przekora A, Ginalska G. In vitro evaluation of the risk of inflammatory response after chitosan/HA and chitosan/ β -1,3-glucan/HA bone scaffold implantation. *Mater Sci Eng C Mater Biol Appl*. 2016;61:355–361. doi:10.1016/j.msec.2015.12.066
27. Götz W, Gerber T, Michel B, Lossdörfer S, Henkel KO, Heinemann F. Immunohistochemical characterization of nanocrystalline hydroxyapatite silica gel (NanoBone(r)) osteogenesis: a study on biopsies from human jaws. *Clin Oral Implants Res*. 2008;19:1016–1026. doi:10.1111/j.1600-0501.2008.01569.x
28. Jensen SS, Yeo A, Dard M, Hunziker E, Schenk R, Buser D. Evaluation of a novel biphasic calcium phosphate in standardized bone defects: a histologic and histomorphometric study in the mandibles of minipigs. *Clin Oral Implants Res*. 2007;18:752–760. doi:10.1111/j.1600-0501.2007.01417.x
29. Ghanaati S, Barbeck M, Detsch R, et al. The chemical composition of synthetic bone substitutes influences tissue reactions in vivo: histological and histomorphometrical analysis of the cellular inflammatory response to hydroxyapatite, beta-tricalcium phosphate and biphasic calcium phosphate ceramics. *Biomed Mater*. 2012;7:e015005. doi:10.1088/1748-6041/7/1/015005
30. Denry I, Kuhn LT. Design and characterization of calcium phosphate ceramic scaffolds for bone tissue engineering. *Dent Mater*. 2016;32:43–53. doi:10.1016/j.dental.2015.09.008
31. Wang J, Chen Y, Zhu X, et al. Effect of phase composition on protein adsorption and osteoinduction of porous calcium phosphate ceramics in mice. *J Biomed Mater Res A*. 2014;102:4234–4243. doi:10.1002/jbm.a.35102
32. Tang D, Tare RS, Yang LY, Williams DF, Ou KL, Oreffo RO. Biofabrication of bone tissue: approaches, challenges and translation for bone regeneration. *Biomaterials*. 2016;83:363–382. doi:10.1016/j.biomaterials.2016.01.024
33. da Silva Brum I, Frigo L, Lana devita R, da Silva Pires JL. Histomorphometric, immunohistochemical, ultrastructural characterization of a nano-hydroxyapatite/beta-tricalcium phosphate composite and a bone xenograft in sub-critical size bone defect in rat calvaria. *Materials*. 2020;13:4598. doi:10.3390/ma13204598
34. Michiel Croes F, Oner C, Kruyt MC. Proinflammatory mediators enhance the osteogenesis of human mesenchymal stem cells after lineage commitment. *PLoS One*. 2015;10(7):e0132781. doi:10.1371/journal.pone.0132781
35. Maruyama M, Rhee C, Utsunomiya T, Zhang N, Ueno M. Modulation of the inflammatory response and bone healing. *Front Endocrinol (Lausanne)*. 2020;11:386. doi:10.3389/fendo.2020.00386
36. Salhotra A, Shah HN, Levi B, Longaker MT. Mechanisms of bone development and repair. *Nat Rev Mol Cell Biol*. 2020;21(11):696–711. doi:10.1038/s41580-020-00279-w

International Journal of Nanomedicine

Dovepress

Publish your work in this journal

The International Journal of Nanomedicine is an international, peer-reviewed journal focusing on the application of nanotechnology in diagnostics, therapeutics, and drug delivery systems throughout the biomedical field. This journal is indexed on PubMed Central, MedLine, CAS, SciSearch®, Current Contents®/Clinical Medicine,

Journal Citation Reports/Science Edition, EMBase, Scopus and the Elsevier Bibliographic databases. The manuscript management system is completely online and includes a very quick and fair peer-review system, which is all easy to use. Visit <http://www.dovepress.com/testimonials.php> to read real quotes from published authors.

Submit your manuscript here: <https://www.dovepress.com/international-journal-of-nanomedicine-journal>